Carbohydrate Research, 166 (1987) 181–193
Elsevier Science Publishers B.V., Amsterdam – Printed in The Netherlands

A SEMIEMPIRICAL THEORY OF THE OPTICAL ACTIVITY OF SACCHARIDES

EUGENE S. STEVENS* AND BANLACORE K. SATHYANARAYANA
Department of Chemistry, University Center at Binghamton, State University of New York, Binghamton, New York 13901 (U.S.A.)

(Received January 3rd, 1987; accepted for publication in revised form, March 14th, 1987)

ABSTRACT

A semiempirical theory of optical activity of saccharides is developed that (*a*) goes beyond previous empirical treatments, (*b*) yields calculated Na_D rotations which correlate well with experimental data, and (*c*) accounts for a characteristic c.d. band observed for polysaccharides in the vacuum u.v. spectrum.

INTRODUCTION

There has been no explanation of the optical activity of polysaccharides in terms of their electronic transitions, undoubtedly because those transitions occur in the vacuum ultraviolet (v.u.v.) region of the spectrum, which has only recently become accessible to experimental measurements. V.u.v. circular dichroism (c.d.) measurements have now been carried out on a great many polysaccharides[1,2], revealing a characteristic c.d. band near 150 nm that consistently has the same sign as the observed optical rotatory dispersion (o.r.d.). In two cases that have been analyzed in detail[3,4], it has been shown that the 150-nm c.d. band accounts for much, if not all, of the o.r.d. Other c.d. bands, in the range of 160–185 nm, observed for polysaccharides[1,2] and saccharide monomers[5,6] are too weak, and often of the wrong sign, to account for the o.r.d.†.

A related, but much older, experimental observation is that the o.r.d. of saccharides can be fitted with a one-term Drude equation using a single wavelength parameter of[7] ~150 nm. These experimental data indicate that the c.d. bands responsible for the observed o.r.d. lie far in the vacuum ultraviolet, and there is some indication that the region near 150 nm is perhaps especially important.

It is timely to attempt to develop a theoretical model to account for these observations. *Ab initio* calculations on molecules as large and flexible as saccharides

*To whom correspondence should be addressed.
†The Kronig–Kramers transform of those c.d. bands yields only a small part of the observed Na_D rotation.

0008-6215/87/$ 03.50

are not practical, in spite of the significant progress in applying those methods to calculating the c.d. of somewhat smaller molecules[8]. Our aim here is to propose a semiempirical theory meeting the requirements that (*a*) it include explicit reference to the high-energy electronic transitions which determine optical activity (*b*) the interaction among these transitions be so described as to include dependence on molecular structure, and (*c*) it be sufficiently tractable to allow treatment of polysaccharides. We specifically aim to go beyond purely empirical treatments of saccharide optical activity[9-13], and also beyond simple polarizability theory[14-19].

An approach that satisfies all of the foregoing requirements is to modify polarizability theory by making explicit reference to the high-energy, electric-dipole-allowed transitions that determine polarizability, and then to couple them with perturbation theory (*i.e.*, exciton theory[20]). In this first report, it will be shown that such a treatment results in a characteristic vacuum u.v. c.d. band near 150 nm, and that the magnitude of that band is sufficiently large to account for the o.r.d. observed. Success of the treatment is demonstrated in terms of a correlation between calculated and observed Na_D rotations for monosaccharides.

CALCULATIONAL METHOD

We aim to calculate rotational strengths and the Na_D rotation arising from the set of high-energy, electronic transitions associated with the electrons of all CC, CO, and CH bonds. [Hydroxyl hydrogen atoms are not included; the CO hydroxyl parameters incorporate OH contributions.] We take the transitions to be initially degenerate. Then, for a collection of N exciton states, labeled $k = 1, 2, \ldots N$, the rotational strength associated with each exciton component, R_k, is given[20] by

$$\begin{aligned} R_k &= \mathrm{Im}\ \boldsymbol{\mu}_k \cdot \mathbf{m}_k \\ &= \mathrm{Im}\Big[\sum_{j=1}^{N} C_{jk}\boldsymbol{\mu}_j\Big]\cdot\Big[\sum_{j=1}^{N} C^*_{jk}(\pi\nu^0 i/c)(\mathbf{r}_j \times \boldsymbol{\mu}_j)\Big] \end{aligned} \tag{1}$$

where $\boldsymbol{\mu}_k$ and $\mathbf{m}_k$ are, respectively, the perturbed electric and magnetic transition dipole-moments associated with exciton component k; $\boldsymbol{\mu}_j$ is the jth unperturbed electric-transition dipole-moment; $\mathbf{r}_j$ is the vector from an arbitrary origin to the center of the jth transition-moment, taken as the center of the bond; ν^0 is the unperturbed transition frequency; and c is the speed of light.

The total transition density of each bond is described with three transition moments, $\boldsymbol{\mu}_j$; one polarized along the bond axis and two polarized perpendicular to the bond and to each other. The values of total transition density for CC and CH bonds were taken from Raymonda and Simpson[21], as subsequently modified by Raymonda[22,23]. No literature value is available for the CO bond; C–O(hydroxyl) and C–O(ring) transition-moments were arbitrarily set at 1.5 and 1.4 times the C–C

moment, respectively, with the C–O(hydroxyl) parameter also representing contributions from O–H bonds not included explicitly.

The μ_j values for each bond were calculated from bond polarizability anisotropies, $\alpha_{\parallel}/\alpha_{\perp}$, using the following relations:

$$\mu^2 = \mu_{\parallel}^2 + 2\mu_{\perp}^2 \tag{2}$$

and

$$\mu_{\parallel}^2/\mu_{\perp}^2 = \alpha_{\parallel}/\alpha_{\perp} \tag{3}$$

Anisotropies for CC and CH bonds have been reported by Denbigh[24], Lefevre[25], and Amos and Crispen[26]. Lefevre's value for the CC bond (3.7) is not much different from the average value of the three sets (5.4); Denbigh's value and Amos and Crispen's value are, respectively, larger and smaller than Lefevre's value. For the CH bond, the three values are similar (1.0–1.8). We adopted the average values as our "canonical" parameters (see Table I), but determined the effect of using each of the three sets separately (see Results and Discussion). We initially set the CO bond anisotropies equal to the CC anisotropy, but treated those values as adjustable parameters. The resulting μ_j values are summarized in Table I.

The symbol ν^0 represents the natural frequency of these transitions for an isolated bond, taken here to be 1.43×10^5 cm^{-1} (70 nm). Raymonda and Simpson[21] originally assigned to this frequency a value of 1.09×10^5 cm^{-1} for CC and CH bonds; modification by Raymonda[22] led to values of 1.16×10^5 cm^{-1} for CC bonds, and 0.96×10^5 cm^{-1} for CH bonds. Our use of the higher value is discussed later.

The coefficients, C_{ik}, of eqn. *1* are obtained from the secular equation[20]

$$\sum_{i=1}^{N} C_{ik}(V_{ij} - E_k\delta_{ij}) = 0 \qquad j = 1,2 \ldots N, \tag{4}$$

where V_{ij} is the coulombic interaction-energy of transition moments μ_i and μ_j. We

TABLE I

PARAMETERS FOR THE CALCULATION OF CIRCULAR DICHROISM OF SACCHARIDES[a]

Bond	$\mu(D)$	$\alpha_{\parallel}/\alpha_{\perp}$	$\mu_{\parallel}(D)$	$\mu_{\perp}(D)$
C–C	2.35	5.45	2.01	0.86
C–H	1.15	1.35	0.73	0.63
C–O(hydroxyl)	3.50	5.45	3.00	1.28
C–O(ring)	3.25	6.00	2.81	1.15

[a]See text for method of selection. $\nu^0 = 1.43 \times 10^5$ cm^{-1} ($\lambda^0 = 70$ nm); $\Delta = 5000$ cm^{-1}.

used the distributed monopole method of approximation, in which each transition dipole is represented by a pair of oppositely signed point-charges. Their separation was fixed at 0.2 Å and magnitudes were so assigned as to give the required transition moment, $|\mu_i| = q_i d$, with $d = 0.2$ Å.

Evaluation of eqn. *1* for a fragment containing n bonds gives $N = 3n$ exciton components, and N rotational strengths, R_k. The exciton components are distributed over a range of wavelength determined by the interaction potential (eqn. *4*). A sum rule is obeyed such that

$$\sum_{k=1}^{N} R_k = 0.$$

We specify a Gaussian envelope with bandwidth, Δ_k, and calculate the circular dichroism (molar ellipticity) as a function of wavelength[27].

$$[\theta_k(\lambda)] = [\theta_k^0] \exp [-(\lambda - \lambda_k^0)^2/\Delta_k^2] \tag{5}$$

where Δ_k is the bandwidth and $[\theta_k^0]$ is the ellipticity at the wavelength of exciton component k, λ_k^0,

$$[\theta_k^0] = (48\pi^{3/2}N^0\lambda_k^0 R_k)/(hc\Delta_k) \tag{6}$$

where N^0 is the Avogadro number and h is the Planck constant. With R_k in units of Debye–Bohr magnetons, $[\theta_k(\lambda)]$ has units of deg.cm^2.dmol^{-1}. We chose $\Delta_k = 5000$ cm^{-1}, but the results are not strongly dependent on its value (see later).

The circular dichroism is summed over exciton components

$$[\theta(\lambda)] = \sum_{k=1}^{N} [\theta_k(\lambda)] \tag{7}$$

and the Kronig–Kramers transform yields the optical rotatory dispersion,

$$[\phi(\lambda)] = (2/\pi) \int_0^\infty [\theta(\lambda)] (\lambda'/\lambda^2 - \lambda'^2) d\lambda' \tag{8}$$

The integral in eqn. *8* was evaluated numerically using intervals of 1.0 nm. Eqn. *8* evaluated at 589 nm is the Na_D molar rotation, $[M]_D$.

We also calculated dipole strengths and absorption spectra from the following equations[20,27].

$$D_k = \boldsymbol{\mu}_k \cdot \boldsymbol{\mu}_k = [\sum_{j=1}^{N} C_{jk}\boldsymbol{\mu}_j] \cdot [\sum_{j=1}^{N} C^*_{jk}\boldsymbol{\mu}_j] \tag{9}$$

$$\varepsilon_k(\lambda) = \varepsilon_k^0 \exp[-(\lambda - \lambda_k^0)^2/\Delta_k^2] \tag{10}$$

$$\varepsilon_k^0 = (8/3)(\pi^{5/2} N^0 \lambda_k^0 D_k)/(2.303 \times 10^3 hc\Delta_k) \tag{11}$$

$$\varepsilon(\lambda) = \sum_{k=1}^{N} \varepsilon_k(\lambda) \tag{12}$$

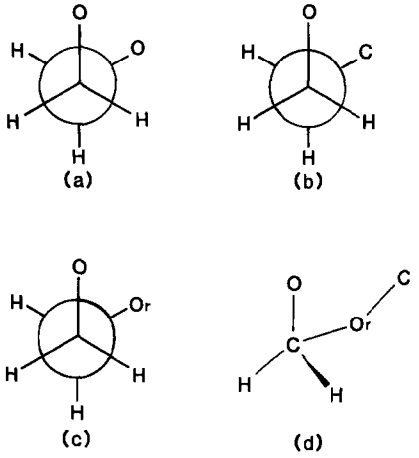

Fig. 1. Fragments used in the calculation of saccharide Na_D rotations. See text and footnote* for details. In (c) and (d), O_r indicates a ring-oxygen atom.

In this first application, we have carried out calculations on the saccharide fragments shown in Fig. 1. These fragments are the ones used in several empirical treatments of saccharide optical activity[11–13] in which the total rotation is successfully represented as a sum of fragment contributions. Fragment **a**, common to all empirical treatments, includes two oxygen atoms in *gauche* relationship across a C–C bond. Fragment **b** includes carbon and oxygen atoms in *gauche* relationship

*Fragment **a** represents Whiffen's fragment[11] *F*, Brewster's term[12] *k*(OH)(OH), and Lemieux's term[13] O/O. Whiffen made a distinction for the case in which one of the oxygen atoms is the glycosidic oxygen atom, yielding an additional parameter *G*. Fragment **b** represents Whiffen's structure *H*, Brewster's *k*(CH)(OH), and Lemieux's O/C. Whiffen and Brewster included an additional empirical parameter for the contribution from the CH_2OH group of hexoses. Lemieux described that contribution as a combination of O/O and O/C terms; to do so, he specified particular rotational isomers of the hydroxymethyl group in a given molecule, *gg*, *gt*, or *tg*, in applying his method. Pyranoses are thereby described by four parameters in Lemieux's method, five in Brewster's, and six in Whiffen's. Pyranosides, not considered in the present work, require an additional parameter. As the point of departure for our semiempirical calculations, we emphasize the significant success of all empirical treatments.

across a C–C bond. Values assigned to fragments **a** and **b** are similar in the various empirical treatments, ~45–55° for fragment **a** and 34–50° for fragment[11–13,*] **b**. Fragments **c** and **d** contain the ring-oxygen atom. The parameters associated with the ring-oxygen atom are larger than those associated with fragments **a** and **b** in all empirical treatments, but the descriptions of the origin of this enhancement differ significantly among the empirical treatments. In our polarizability model, we allow for a distinction between hydroxyl and ring oxygen atoms by adopting different polarizability parameters for them. Standard bond-lengths were used [r(CC) = 1.53 Å, r(CO) = 1.40 Å, and r(CH) = 1.10 Å] together with tetrahedral bond-angles.

These parameters describe the "canonical" set. Systematic variation of parameters allowed a measure of the dependence of calculated results on their values.

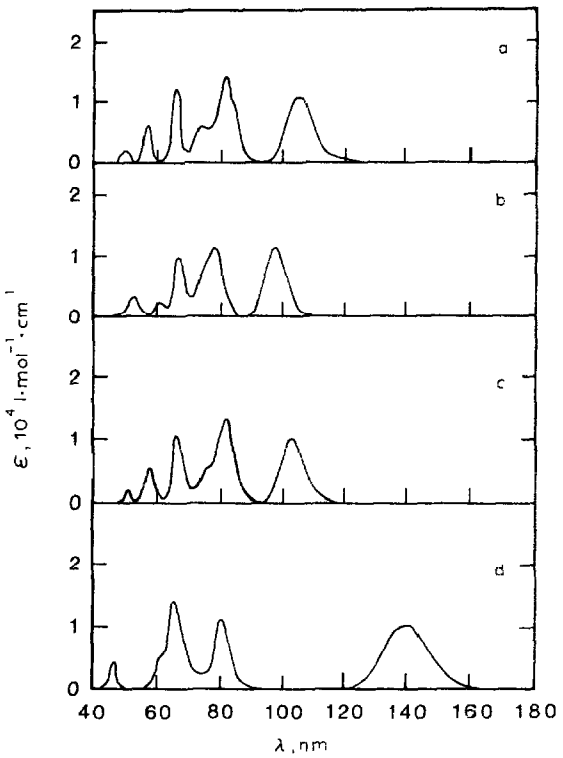

Fig. 2. Calculated absorption spectra of fragments **a**, **b**, **c**, and **d**.

*The calculations refer to molecules (or fragments) in a vacuum. For comparison with solution data, a solvent-correction term should be included, but the correction needed is not well known. One approximation uses the solvent index of refraction, n, in which case, all calculated rotations would be multiplied by $(n^2 + 2)/3$, which is equal to 1.26 for water.

RESULTS

Figure 2 shows the calculated absorption spectra for fragments **a–d**. The most significant feature of the spectra is the appearance of a low-energy-absorption component well separated from the remaining components. In fragments **a, b,** and **c** the low-energy component appears near 100 nm; in fragment **d** it appears near 140 nm. The remaining absorption intensity in each case is distributed about $\lambda^0 = 70$ nm. The low energy absorption component has a well defined polarization; in fragment **a** it is polarized parallel to a vector connecting the oxygen atoms.

Varying the parameter values does not change this basic pattern. Using Lefevre's CC and CH polarizability anisotropies, rather than average values, gave only slightly different results. Denbigh's large CC bond anisotropy typically resulted in a very large exciton splitting, such that the low-energy absorption component appeared, unrealistically, above 200 nm. Amos and Crispen's values[26] gave, as expected, smaller splittings, smaller c.d. bands, and smaller Na_D rotations. Transition moments, μ, for C–O(hydroxyl) and C–O(ring) bonds were systematically varied in the range from 1.0 to 4.0 Debyes, and polarizability anisotropies for those bonds were varied in the range from 1.0 to 10.0. A low-energy absorption-exciton component consistently appears, as in Fig. 2c, but its position varies between 93 and 111 nm. With a shift in λ^0 from 70 to 50 nm, that absorption component shifts from 103 to 66 nm; with $\lambda^0 = 90$ nm, the component appears at 158 nm (*i.e.*, the shift is linear on a frequency scale). Thus, a change in

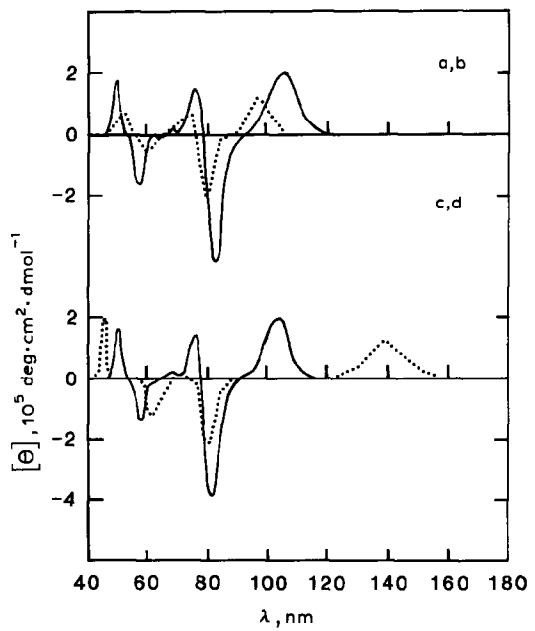

Fig. 3. Calculated circular dichroism spectra of fragments. Solid lines, **a** and **c**; dotted lines, **b** and **d**.

λ^0 results in a simple shift of the entire absorption spectrum, and increasing any of the μ_j values results in a larger splitting between the position of the low-energy absorption-band and λ^0, by virtue of increased terms V_{ij} in the interaction matrix.

This feature of the model places constraints on the parameters λ^0 and μ_j, because it is known from the experimental c.d. spectra[5,6] that the c.d. bands responsible for Na_D rotation occur below 165 nm.

Figure 3 shows the calculated c.d. spectra for fragments **a**, **b**, **c**, and **d**. The high-energy region of the calculated spectra is complex, and the detailed structure in that region cannot be assigned special significance. We do, however, attribute significance to the well separated, positive c.d. band that appears at the same wavelength as the low-energy absorption-component for all four fragments (compare Figs. 2 and 3). Varying the parameter values does not change this basic feature (see earlier).

The position and intensity of the low-energy c.d. band largely determines the magnitude of the calculated Na_D rotation, $[M]_D$. Table II summarizes the values of $[M]_D$ calculated for each fragment by using the canonical set of parameters, and gives the results of adjusting parameters. In general, the canonical set of parameters results in the maximum $[M]_D$ obtainable with the model, given the constraints already described. The calculated values of $[M]_D$ are small compared with the corresponding empirical values, but the contribution of fragment **d** is significantly larger than that of **a** and **b**.

Figure 4 shows the correlation between saccharide Na_D rotation obtained by summing calculated fragment contributions, and experimentally observed Na_D rotations. The correlation indicates that the model reproduces the same dependence of Na_D rotation on chemical structure as is observed experimentally. Quantitatively, however, the calculated Na_D rotations are consistently too low. This discrepancy does not come from the method of summing fragment contribu-

TABLE II

CALCULATED $[M]_D$ FOR FRAGMENTS **a**, **b**, **c**, AND **d** OF Fig. 1 AND DEPENDENCE OF CALCULATED $[M]_D$ ON PARAMETERS

Parameters[a]	*Calc.* $[M]_D$ *(deg.cm².dmol⁻¹)*			
	Fragment a	*Fragment b*	*Fragment c*	*Fragment d*
Canonical set (see Table I)	+13	+4	+11	+29
$\Delta = 7000\ cm^{-1}$	+13	+4	+11	+31
$\Delta = 2000\ cm^{-1}$	+13	+4	+11	+29
$\nu^0 = 1.67 \times 10^5\ cm^{-1}$ ($\lambda^0 = 60$ nm)	+8	+3	+7	+19
μ(C–O)(hydroxyl) = 3.00 D	+6	+3	+8	+18
μ(C–O)(ring) = 3.00 D	+9	+3	+9	+18
$\alpha_\parallel/\alpha_\perp$(C–O)(hydroxyl) = 1.0	+1	+1	+2	+5
$\alpha_\parallel/\alpha_\perp$(C–O)(ring) = 1.0	+2	+1	+2	+1

[a]In each case, parameters were those of the canonical set, except for the single parameter indicated.

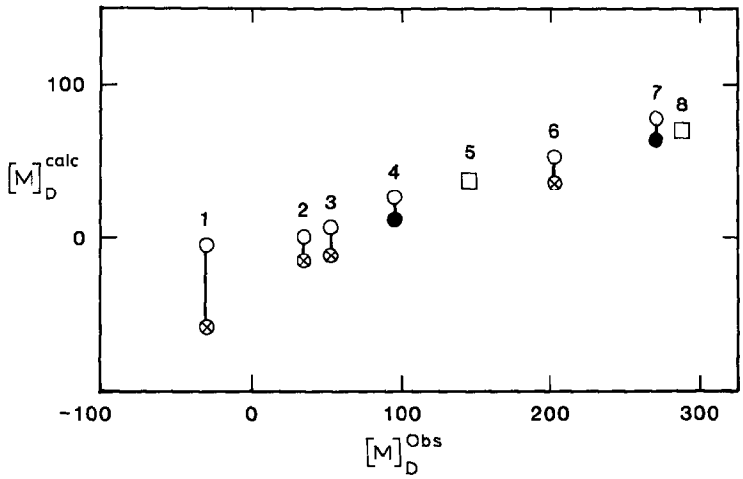

Fig. 4. Correlation of saccharide Na_D rotations obtained by summing calculated fragment contributions ($[M]_D^{calc}$) and experimental values ($[M]_D^{obs}$). (1) β-D-Mannose; (2) β-D-glucose; (3) α-D-mannose; (4) β-D-galactose; (5) α-D-xylose; (6) α-D-glucose; (7) α-D-galactose; and (8) β-L-arabinose. ○, *gt*; ⊗, *gg*; ●, *tg*. Units are deg.cm^2.dmol^{-1}.

tions which we use to evaluate the model, as a test calculation on α-D-glucose (19 bonds) gave approximately the same Na_D rotation as the summed calculated fragment contributions.

DISCUSSION

The ability of the model to reproduce the same dependence of Na_D rotation on chemical structure as is observed (see Fig. 4) must be taken as indicating its fundamental viability. This qualitative agreement with experiment arises essentially because the model produces a low-energy c.d. band of proper sign and magnitude. This feature does not depend on values assigned to parameters (see earlier), but is inherent in the model.

The absorption spectra can be understood qualitatively in terms of the local C_2 symmetry in fragments **a**–**d**. For example, the symmetry axis of fragment **a** is perpendicular to the C–C bond and bisects the angle between the projections of the C–O bonds on a plane perpendicular to the C–C bond. The lowest-energy absorption component of fragment **a** is polarized entirely perpendicular to its symmetry axis and parallel to a vector connecting the oxygen atoms, identifying it as belonging to the $B(x,y)$ irreducible representation of the C_2 point group. Replacing the two oxygen atoms of fragment **a** with hydrogen atoms yields ethane in its staggered conformation, and, referring back to the D_{3d} point group of staggered ethane, it is found that the $B(x,y)$ irreducible representation of the C_2 point group correlates with the $E_u(x,y)$ irreducible representation of the D_{3d} point group. Ethane itself is known to show a well separated low-energy absorption band

near 135 nm[21], and a Pariser–Parr calculation by Katagiri and Sandorfy[28] indicates the first electronic transition in ethane to correspond to $A_{1g} \rightarrow E_u$. In these terms, we attribute the well separated low-energy absorption component, found in all four fragments (see Fig. 2), to the approximately D_{3d} symmetry of saccharide fragments containing tetrahedral carbon atoms in a puckered ring.

Similarly, the positive sign of the rotational strength of the low-energy exciton component results from the relative magnitude of transition moments associated with the CC, CH, and CO groups. In fragment **a**, for example, the low-energy c.d. band is positive because the transition moments associated with the CO bond are greater than those associated with the CH bond. The result that fragment **a** is dextrorotatory is, of course, consistent with other well known descriptions of optical activity, such as Kauzmann's helical model[29] and Brewster's application of it to skewed conformational units[30]. Detailed analysis of the results for fragment **a** showed that the magnetic transition moment associated with the low-energy exciton component is polarized entirely in the plane perpendicular to the CC bond, and it is the scalar product of that moment and the electric transition moment (see earlier) that determines the sign of the low-energy c.d. band (see Eqn. *1*). As the sign of the low-energy c.d. band determines the sign of the Na_D rotation, the qualitative success of the model is inherent to the model and is not an accident of parameterization.

The characteristic 150-nm c.d. band observed for polysaccharides[1-4] may well reflect this feature of local symmetry. The calculated fragment c.d. spectra (see Fig. 3) shows $[\theta^0]$ values on the order of 10^5 deg.cm^2.dmol^{-1}. Values extracted from experimental c.d. data are of the same order of magnitude, *e.g.*, $+0.8 \times 10^5$ deg.cm^2.dmol^{-1} for the (1→6)-linked polymer of α-D-galactose and -0.3×10^5 deg.cm^2.dmol^{-1} for the (1→4)-linked polymer of β-D-mannose[3].

The two- to three-fold discrepancy between calculated and observed rotations we find here is not uncommon in attempts to calculate optical activity. In the present model, part of the discrepancy is likely to come from the use of Kirkwood's polarizability theory of optical activity[14,15]. The fundamental approximation in that theory is to decompose the molecular optical activity into contributions from component groups, and to take the phase of the incident light as being equal at every point in a given group. We have evaluated the coupling retained by this approximation, the $\boldsymbol{\mu}$–$\boldsymbol{\mu}$ coupling. Omitted is the so-called $\boldsymbol{\mu}$–$\mathbf{m}$ coupling between electric-dipole transition moments and intrinsic magnetic-dipole transition moments. In a recent *ab initio* calculation of the optical activity of methyl derivatives of cyclopropane, Bohan and Bouman[8] found the $\boldsymbol{\mu}$–$\boldsymbol{\mu}$ coupling to make, consistently, the largest contribution to rotational strength, but the $\boldsymbol{\mu}$–$\mathbf{m}$ coupling contribution, in the cases examined, were of the same sign and order of magnitude.

Even within the framework of polarizability theory, the approximations that we chose to make may also account for part of the discrepancy. We enumerate these here in the order of their probable importance.

(*1*) Exciton theory has often been applied to polymers in the framework of a

group-separability approximation (neglecting electron exchange), where the interacting transitions are on adjoining monomer units and thus separated, typically, by two bonds several Ångström units apart. Precedents exist, however, for applying it to transitions on adjoining bonds, as is done here. Bowman *et al.*[23] successfully accounted for some features of the vacuum u.v. c.d. of cyclic amides by coupling σ–σ^* transitions on adjoining bonds, using a method essentially the same as ours. They, in turn, had noted Raymonda and Simpson's earlier successful application of exciton theory to σ–σ^* transitions in explaining trends in alkane absorption spectra[21]. These two previous successful applications motivated the present use of exciton theory to couple transitions on neighboring bonds, but the inadequacy of our approximation of the matrix elements, V_{ij}, is possibly a significant source of error.

(*2*) We excluded explicit consideration of the hydroxyl hydrogen atoms, largely because of the difficulty in treating the rotation of hydroxyl groups about OC bonds. An alternative would be to include, explicitly, OH transition moments centered on a vector parallel to the CO bond but beyond the oxygen atom, so as to mimic an averaged OH-bond position.

(*3*) A single value of λ^0 was used for all bonds. The qualitative success of the results reflects the fact that the calculated property of interest, *i.e.*, the Na_D rotation, is far removed from the resulting exciton components, but quantitative improvement may require the assigning of different λ^0 values for each type of bond, *i.e.*, CC, CH, CO(hydroxyl), and CO(ring).

(*4*) We partitioned total transition intensities into components parallel and perpendicular to the bond by using bond-polarizability anisotropies extracted from group additive polarizability models. Such models have properly been criticized (*e.g.*, in ref. 16) and, even within the framework of an additivity model, there is substantial uncertainty in appropriate anisotropy parameters[24,25]. We were therefore careful to vary the anisotropy parameters sufficiently to show that the qualitative features of our results are independent of the particular values chosen (see earlier).

(*5*) Likely of lesser importance are the dependence of results on the precise geometry of the fragments, the use of a gaussian bandshape, and, as we have shown, the bandwidth of the exciton components (Table II).

The present model has its roots in Kirkwood's polarizability theory of optical activity[14,15], which in turn is closely related to the coupled oscillator model of Kuhn[31,32]. Indeed, if the ultimate objective of this study had been merely a rationalization of observed Na_D molar ratations, the use of simple polarizability theory would have been more appropriate. For example, Applequist and coworkers[16] developed a procedure for calculating molecular polarizabilities by using an all-order dipole interaction model, and applied that model to calculate Na_D rotations[17] for the same cyclohexane polyols that Whiffen[11] originally used to extract his empirical contribution for fragment **a** [+45°]. Applequist *et al.*[16] obtained results that were of the proper sign but that were too large by a factor of ~2. Refinements

in the dipole interaction model[18,19] might result in improved optical rotation values, and the method can clearly be applied to saccharides as well.

Our model is, however, derived from a polarizability theory in which the electric dipole allowed transitions deep in the vacuum u.v., presumed to be the dominant source of rotational strength in polarizability theory, are made explicit, and then are coupled with an exciton formalism. The conceptual advantage of the model is its representation of the Na_D rotation as the net effect of a relatively simple pattern of c.d. bands deep in the vacuum u.v. Also, if the wavelength range of current vacuum-u.v. c.d. instruments can be extended, the saccharide c.d. bands responsible for the Na_D rotation, which we have attempted to calculate here, will be directly observable.

Because the parameterization required in the present model is partly derived from bond polarizability anisotropies, all-order polarizability theory may eventually provide guidance in developing an improved parameterization. The original version of the theory[16] was not as successful in calculations of anisotropies as it was in calculation of average molecular polarizabilities, but this deficiency was partially removed by refinements[18,19]. However, to be useful in our model, current all-order polarizability theories would have to be recast, using bonds instead of atoms as the polarizable units.

CONCLUSIONS

A semiempirical model of saccharide optical activity has been constructed by combining a modified polarizability theory with an exciton coupling mechanism. Exciton-like features appear in the calculated absorption and circular dichroism spectra, and the resulting Na_D rotations for a series of monosaccharides correlate well with experimental values.

ACKNOWLEDGMENT

This work was partially supported by NSF Grant CHE 85-09520 and NIH Grant GM24862.

REFERENCES

1 E. S. STEVENS, in F. ALLEN AND C. BUSTAMANTE (Eds.), *Applications of Circularly Polarized Radiation Using Synchrotron and Ordinary Sources*, Plenum, New York, 1985, pp. 173–189.
2 E. S. STEVENS, *Photochem. Photobiol.*, 44 (1986) 287–293.
3 L. A. BUFFINGTON, E. S. STEVENS, E. R. MORRIS, AND D. A. REES, *Int. J. Biol. Macromol.*, 2 (1980) 199–203.
4 E. R. MORRIS, E. S. STEVENS, S. A. FRANGOU, AND D. A. REES, *Biopolymers*, 25 (1986) 959–973.
5 R. G. NELSON AND W. C. JOHNSON, JR., *J. Am. Chem. Soc.*, 98 (1976) 4290–4295.
6 R. G. NELSON AND W. C. JOHNSON, JR., *J. Am. Chem. Soc.*, 98 (1976) 4296–4301.
7 T. M. LOWRY, *Optical Rotary Power*, Dover, New York, 1964.
8 S. BOHAN AND T. D. BOUMAN, *J. Am. Chem. Soc.*, 108 (1986) 3261–3266
9 E. FISCHER, *Ber.*, 28 (1895) 1145–1167.

10 C. S. HUDSON, *J. Am. Chem. Soc.*, 47 (1925) 268–280.
11 D. H. WHIFFEN, *Chem. Ind. (London)*, (1956) 964–968.
12 J. H. BREWSTER, *J. Am. Chem. Soc.*, 81 (1959) 5483–5493.
13 R. U. LEMIEUX AND J. T. BREWER, *Adv. Chem. Ser.*, 117 (1973) 121–146.
14 J. G. KIRKWOOD, *J. Chem. Phys.*, 5 (1937) 479–491.
15 J. G. KIRKWOOD, *J. Chem. Phys.*, 7 (1939) 139.
16 J. APPLEQUIST, J. R. CARL, AND K.-K. FUNG, *J. Am. Chem. Soc.*, 94 (1972) 2952–2960.
17 J. APPLEQUIST, *J. Am. Chem. Soc.*, 95 (1973) 8258–8262.
18 B. T. THOLE, *Chem. Phys.*, 59 (1981) 341–350.
19 R. R. BIRGE, G. A. SCHICK, AND D. F. BOCIAN, *J. Chem. Phys.*, 79 (1983) 2256–2264.
20 I. TINOCO, R. W. WOODY, AND D. F. BRADLEY, *J. Chem. Phys.*, 38 (1963) 1317–1325.
21 J. W. RAYMONDA AND W. T. SIMPSON, *J. Chem. Phys.*, 47 (1957) 430–448.
22 J. W. RAYMONDA, personal communication cited in ref. 23.
23 R. L. BOWMAN, M. KELLERMAN, AND W. C. JOHNSON, JR., *Biopolymers*, 22 (1983) 1045–1070.
24 K. G. DENBIGH, *Trans. Faraday Soc.*, 36 (1940) 936–948.
25 R. J. W. LEFEVRE, *Adv. Phys. Org. Chem.*, 3 (1965) 1–90.
26 A. T. AMOS AND R. J. CRISPEN, *J. Chem. Phys.*, 63 (1975) 1890–1899.
27 A. MOSCOWITZ, in C. DJERASSI (Ed.), *Optical Rotatory Dispersion*, McGraw–Hill, New York, 1950, pp. 150–177.
28 S. KATAGIRI AND C. SANDORFY, *Theor. Chim. Acta*, 4 (1966) 203–223.
29 W. KAUZMANN, *Quantum Chemistry*, Academic Press, New York, 1957.
30 J. H. BREWSTER, *Top. Stereochem.*, 2 (1967) 1–72.
31 W. KUHN, *Z. Phys. Chem., Abt. B*, 4 (1929) 14–36.
32 W. KUHN, *Trans. Faraday Soc.*, 26 (1930) 293–308.